



Cite this: *Phys. Chem. Chem. Phys.*,
2016, **18**, 11150

Effects of CO and CO₂ on the desulfurization of H₂S using a ZnO sorbent: a density functional theory study†

Lixia Ling,^{ab} Zhongbei Zhao,^a Baojun Wang,^{*c} Maohong Fan^{*b} and Riguang Zhang^c

The density functional theory (DFT) method has been performed to study the effects of CO and CO₂ on the desulfurization of H₂S over a ZnO sorbent. It shows that COS is inevitably formed on the ZnO(10 $\bar{1}$ 0) surface, which tends to be adsorbed onto the surface via a S–C bond binding with either a long or a short Zn–O bond. Potential energy profiles for the COS formation via reactions between H₂S and CO, and H₂S and CO₂ on the ZnO(10 $\bar{1}$ 0) surface have been constructed. In the presence of CO, the dissociated active S of H₂S reacting with CO leads to the formation of COS, and the activation energy of the rate-determining step is 87.7 kJ mol⁻¹. When CO₂ is present, the linear CO₂ is first transferred to active CO₂ in a triplet state, and then combines with active S to form COS with the highest energy barrier of 142.4 kJ mol⁻¹. Rate constants at different temperatures show that the formation of COS via the reaction of CO and H₂S is easier than that of CO₂ and H₂S over the ZnO surface.

Received 1st March 2016,
Accepted 22nd March 2016

DOI: 10.1039/c6cp01422d

www.rsc.org/pccp

1. Introduction

H₂S in coal-derived gas must be removed, not only because it has severe corrosive properties,^{1–3} but also because it is poisonous to downstream catalysts in synthesizing chemical products such as methanol, diethyl ether, and dimethyl carbonate (DMC).^{4–6} Current research seems to be concentrated on ZnO due to its high desulfurization efficiency and sensitivity to H₂S.^{7–10} However, two main compounds in coal-derived gas, CO and CO₂, obviously affect the removal of H₂S over a ZnO sorbent.

Up to now, certain experimental research efforts have focused on the effects of CO and CO₂ on the desulfurization of H₂S. When CO together with H₂S was fed into a fixed-bed reactor using a zinc-based sorbent, COS formation occurred. The inhibition effect of ZnO on H₂S capture was attributed to the competitive adsorption between H₂S and CO₂ on the ZnO surface.¹¹ A related work was also carried out by Sasaoka *et al.*¹² It can be concluded that COS was found in the outlet gas from the reactor, which was produced via the reaction between active surface sulfur S^{*} and CO. However, elemental sulfur was not observed in the presence of CO₂. Yang *et al.*¹³ also discovered

that both CO and CO₂ reacted with H₂S to form COS, CO homogeneously and CO₂ heterogeneously, on the sulfide surface (ZnS); *i.e.*, H₂S first reacted with ZnO to form ZnS, and then ZnS reacted with CO₂, leading to the formation of COS. COS has also been investigated during the desulfurization of H₂S in the presence of CO using iron oxide sorbents,^{14,15} which may catalyze the reaction between H₂S and CO.¹⁶ The conversion of sulfur-containing species during desulfurization will increase the difficulty in finding an efficient desulfurizer.

A quantum chemistry method has been employed to explore reaction mechanisms aimed at revealing the entire reaction process, thereby clarifying key steps required to either accelerate or decelerate a reaction.¹⁷ Adsorption is the first step for the heterogeneous reaction. Certain theoretical studies have been carried out to investigate the interaction of different gases on the ZnO surface. The adsorption of CO,^{18–22} CO₂,^{22,23} H₂S and its S-containing dissociated species (SH and S)^{24,25} onto the ZnO surface was studied using cluster models, and the stable adsorption structures, adsorption energy and charge change were determined. A periodic model was also adopted to study the adsorption of H₂S, SH and S on the ZnO(0001) surface;²⁶ it can be concluded that these species are strongly adsorbed onto the ZnO surface. However, only the adsorption of single species was studied, with the effects of other gases in coal-derived gas remaining to be considered.

In our previous work, we studied the sulfuration mechanism of H₂S on the ZnO(10 $\bar{1}$ 0) surface during the desulfurization of coal gas,²⁷ the regeneration mechanisms of the sulfurized ZnO(10 $\bar{1}$ 0) surface and oxygen-deficient ZnO(10 $\bar{1}$ 0) surfaces in the presence of O₂,²⁸ and the simultaneous removal mechanism

^a College of Chemistry and Chemical Engineering, Taiyuan University of Technology, Taiyuan 030024, Shanxi, P. R. China. E-mail: linglixia@tyut.edu.cn

^b Department of Chemical and Petroleum Engineering, The University of Wyoming, Laramie, WY 82071, USA. E-mail: mfan@uwyo.edu

^c Key Laboratory of Coal Science and Technology (Taiyuan University of Technology), Ministry of Education and Shanxi Province, Taiyuan 030024, Shanxi, People's Republic of China. E-mail: wangbaojun@tyut.edu.cn

† Electronic supplementary information (ESI) available. See DOI: 10.1039/c6cp01422d

of H_2S and Hg^0 over the ZnO surface.²⁹ In addition, the effects of oxygen deficiency on the adsorption and dissociation of H_2S have been studied.³⁰ However, the essential effects of CO and CO_2 on the reaction between H_2S and ZnO are not clear. In this study, we present a periodic DFT investigation of the adsorption and reaction of H_2S on the $\text{ZnO}(10\bar{1}0)$ surface in the presence of CO and CO_2 , in order to provide a theoretical basis for improving the desulfurization efficiency of H_2S in flue gas.

2. Computational model and method

2.1 Surface model

For the surface model, we examined a $\text{ZnO}(10\bar{1}0)$ surface to study the effects of CO and CO_2 on the desulfurization of H_2S , since $\text{ZnO}(10\bar{1}0)$ is electrostatically stable and theoretically the easiest surface to treat.^{31,32} A $\text{ZnO}(10\bar{1}0)$ surface model with 8 atomic layers and a $p(3 \times 2)$ supercell was constructed, as shown in Fig. 1. Previous theoretical studies have shown that the 8-layer slab model adequately represents the $\text{ZnO}(10\bar{1}0)$ surface.^{33–35} The slab was repeated periodically in the x - y directions with a 12 Å vacuum region between the slabs in the z -direction. Except for the bottom two layers of the slab frozen to bulk positions, all atoms were allowed to relax in all calculations.

2.2 Computational method

Calculations were performed using periodic DFT calculations, for which the generalized gradient approximation (GGA) using the Perdew–Wang 1991 (PW91) functional^{36–38} was chosen. A double numerical plus polarization (DNP) was used as the basis set, with a global orbital cutoff of 4.4 Å. The inner electrons of zinc atoms were kept frozen and replaced by an effective core potential (ECP); other atoms in this study were treated with an all-electron basis set. The k -point sampling scheme of the Monkhorst–Pack grid of $3 \times 2 \times 1$ was chosen.³⁹ All calculations were performed using the Dmol³ program package^{40,41} on a Dell R715 server system. In order to obtain an accurate active barrier of the reaction, a complete LST/QST method⁴² was explored to search for the transition state (TS) at the same theoretical level. Meanwhile, TS confirmation was performed to ensure that every

transition state led to the desired reactant and product, and frequency analysis was used to verify each transition state with only one imaginary frequency.

The activation energy (E_a) for every elemental step and adsorption energies (E_{ads}) of the adsorbate–substrate system are defined as follows:

$$E_a = E(\text{TS}) - E(\text{R}) \quad (1)$$

$$E_{\text{ads}} = E_{\text{adsorbate}} + E_{\text{slab}} - E_{\text{adsorbate/slab}} \quad (2)$$

where $E(\text{TS})$ and $E(\text{R})$ are electronic total energies of the transition state and the reactant, respectively; $E_{\text{adsorbate}}$ and E_{slab} are the electronic total energies of the free adsorbate in the gas phase and the slab, respectively; and $E_{\text{adsorbate/slab}}$ is the electronic total energy of the adsorbate–slab system in the equilibrium state.

3. Results and discussion

3.1 Structure and energetics of adsorbed reactants and products

To investigate the effects of CO and CO_2 on the desulfurization of H_2S on the $\text{ZnO}(10\bar{1}0)$ surface, we first need to know the individual bonding nature of different reactants and the possible products, including the binding mechanism of H_2S , CO , CO_2 , H_2 , H_2O and COS on the $\text{ZnO}(10\bar{1}0)$ surface. Some results have been reported for the adsorption of H_2S , CO , CO_2 , H_2 and H_2O , so only the most stable structures are discussed and compared with previous results. All possible adsorption configurations of COS on the $\text{ZnO}(10\bar{1}0)$ surface are shown and analyzed. The optimized structures are shown in Fig. 2, and the corresponding adsorption energies are listed in Table 1.

H_2S adsorption. The H_2S molecule is dissociatively adsorbed onto the $\text{ZnO}(10\bar{1}0)$ surface with an adsorption energy of 135.1 kJ mol^{-1} , which is only 3.5 kJ mol^{-1} higher than on the $p(2 \times 2)$ slab in our previous studies.^{27,28} The dissociative adsorption agrees with the experimental observation⁴³ and other theoretical results.²⁴ One S–H bond is elongated to 2.077 Å compared to that of a free H_2S molecule (1.354 Å).

CO adsorption. The CO molecule binds with its C end down to the three-fold Zn atom on the surface, but tilts toward the coordinatively unsaturated surface O. θ represents the angle between the normal surface and the molecular axis. The calculated θ for CO adsorption is about 23.9° on the $\text{ZnO}(10\bar{1}0)$ surface, which more reasonably accords with the UPS and ARPES measurements of 30.0°^{44,45} than the other theoretical result of 41.7° with a 4-layer slab model.⁴⁶ The adsorption energy is 40.4 kJ mol^{-1} , which agrees with the experimental value of $50.2 \pm 1.7 \text{ kJ mol}^{-1}$ ⁴⁵ and the other periodic DFT result of 45.6 kJ mol^{-1} .⁴⁶ The bond length of C–O is 1.137 Å, which is close to the similar theoretical result of 1.140 Å.⁴⁶ It can be seen that the result obtained from the DFT method using a periodic model is more reasonable than that obtained using a cluster model or a semiempirical method.

CO_2 adsorption. According to our calculations, a nearly linear geometry and a V-shape geometry are obtained, which are shown as $\text{CO}_2(\text{a})$ and $\text{CO}_2(\text{b})$ in Fig. 2. $\text{CO}_2(\text{a})$ has the most

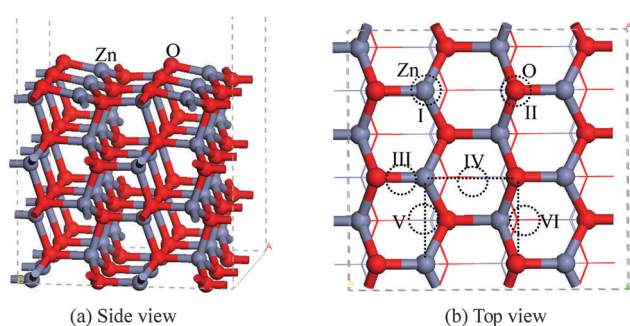


Fig. 1 The slab model of the $\text{ZnO}(10\bar{1}0) - (3 \times 2)$. (a) Side view of the $\text{ZnO}(10\bar{1}0)$ surface; (b) Top view of the $\text{ZnO}(10\bar{1}0)$ surface. I, II, III, IV, V and VI correspond to active sites for “Zn-top”, “O-top”, “short Zn–O bridge”, “long Zn–O bridge”, “Zn–Zn bridge”, and “O–O bridge” sites, respectively. The dotted line represents the supercell used in this study.

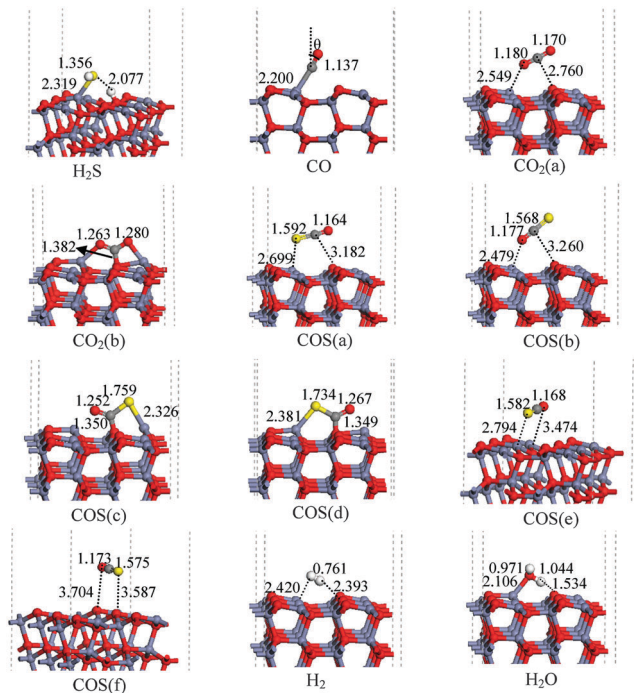


Fig. 2 Adsorption configurations of H_2S , CO , CO_2 , COS , H_2 and H_2O on the $\text{ZnO}(10\bar{1}0)$ surface.

Table 1 The adsorption energies of different species on the $\text{ZnO}(10\bar{1}0)$ surface

Structures	ΔE_{ads} (kJ mol^{-1})	Structures	ΔE_{ads} (kJ mol^{-1})
H_2S	135.1	COS(a)	24.4
CO	40.4	COS(b)	14.2
$\text{CO}_2(\text{a})$	23.3	COS(c)	135.2
$\text{CO}_2(\text{b})$	77.4	COS(d)	124.8
H_2	10.2	COS(e)	15.0
H_2O	101.5	COS(f)	3.9

stable nearly linear geometry. The adsorbed CO_2 molecule presents two different C–O bond lengths of 1.180 Å and 1.170 Å. The larger C–O bond length corresponds to the O_{CO_2} end down to the surface with an adsorption energy of 23.3 kJ mol^{-1} , which is a physical adsorption. A similar configuration has been investigated with a $(\text{ZnO})_{348}$ cluster model by Martins *et al.*,²² with higher adsorption energies of 150.6 kJ mol^{-1} and 51.7 kJ mol^{-1} obtained at 3-21G and 6-31+G** basis set levels, respectively. In $\text{CO}_2(\text{b})$, the CO_2 molecule changes from a linear geometry in gas to a V-shape geometry. The two O atoms bond to two Zn atoms, and the C atom bonds to the surface O atom leading to a carbonate structure. The bond length of C– $\text{O}_{\text{surface}}$ is 1.382 Å and the adsorption energy is 77.4 kJ mol^{-1} . Chen *et al.*²³ have investigated a similar configuration with a $(\text{ZnO})_4$ cluster, obtaining a higher adsorption energy of 139.6 kJ mol^{-1} . It can be seen that CO_2 adsorption on the V-shaped structure is more active than on the linear structure.

COS adsorption. Six side-on modes are optimized by placing COS at “long Zn–O bridge”, “short Zn–O bridge”, “Zn–Zn bridge”, and “O–O bridge” sites with different directions; the

optimized configurations are shown as COS(a) – COS(f) in Fig. 2. COS declines over the long Zn–O bridge site with S and O ends down to the threefold Zn atom in COS(a) and COS(b) with adsorption energies of 24.4 and 14.2 kJ mol^{-1} , respectively. In COS(c) , COS is adsorbed onto the $\text{ZnO}(10\bar{1}0)$ surface with the S binding the surface Zn atom and C binding the surface O, and the Zn and O with a short Zn–O bond. The adsorbed COS is V-shaped, with an adsorption energy of 135.2 kJ mol^{-1} . COS(d) has a structure similar to COS(c) , in which COS interacts with the long Zn–O bond with an adsorption energy of 124.8 kJ mol^{-1} . In COS(e) and COS(f) , COS bridges two adjacent Zn atoms with an adsorption energy of 15.0 kJ mol^{-1} and two adjacent O atoms with an adsorption energy of 3.9 kJ mol^{-1} , respectively. Comparing the adsorption energies of the six configurations, we can see that COS prefers to adsorb onto the surface with S binding on the surface Zn, and with C binding on the surface O, which is in line with the results of Aboulayt *et al.*⁴⁷

H_2 adsorption. H_2 is detected as the product when CO together with H_2S is fed into the reactor with ZnO desulfurizer,¹³ such that only the non-dissociative adsorption structure of H_2 on the $\text{ZnO}(10\bar{1}0)$ surface is investigated, which is shown in Fig. 2. The H_2 molecule is adsorbed onto the long Zn–O bridge site with a tilting angle of 61.0°. The H–O and H–Zn bonds are 2.393 and 2.420 Å, respectively. The adsorption energy is 10.2 kJ mol^{-1} , which is in good agreement with the similar theoretical result of 10.3 kJ mol^{-1} using a periodic plane model.⁴⁶

H_2O adsorption. Consistent with previous studies,^{22,24,48,49} we find that the H_2O molecule prefers to adsorb onto a Zn site on the surface, but moves toward the hexagonal channel, so that one H atom of the H_2O molecule is nearly bonded to a nearby oxygen atom on the surface, as indicated in Fig. 2. The distance between the surface O and H in H_2O , marked by the dotted line, is 1.534 Å. The bond length between the O atom of the H_2O molecule and the adsorbing Zn atom is 2.106 Å. The adsorption energy is 101.5 kJ mol^{-1} , which is in accordance with the result of 98.4 kJ mol^{-1} at the 6-31+G** basis set level with a $(\text{ZnO})_{348}$ cluster and the periodic calculated value of 91.7 kJ mol^{-1} .⁴⁹

3.2 The reaction of CO and H_2S

To characterize the reaction pathway of CO and H_2S on the $\text{ZnO}(10\bar{1}0)$ surface, Fig. 3 shows the potential energy profile and the corresponding structures of intermediates and transition states. The imaginary frequency for every transition state during this reaction is listed in Table S1 in the ESI.† The co-adsorption of H_2S and CO on the $\text{ZnO}(10\bar{1}0)$ surface is an exothermic process with an energy of -174.4 kJ mol^{-1} , in which H_2S is dissociated spontaneously and CO binds with the C end down to coordinatively unsaturated Zn. This is the first dehydrogenation step, which leads to the intermediate IM1.

Next, the dissociated SH adsorbs onto the S on two adjacent Zn atoms of the surface in a bridge bonding mode, and the intermediate IM2 is formed through TS1 with the energy barrier of 40.6 kJ mol^{-1} . Subsequently, the second dehydrogenation step takes place by overcoming a reaction barrier of 52.5 kJ mol^{-1} at TS2, producing IM3. In the first two steps, CO always remains the

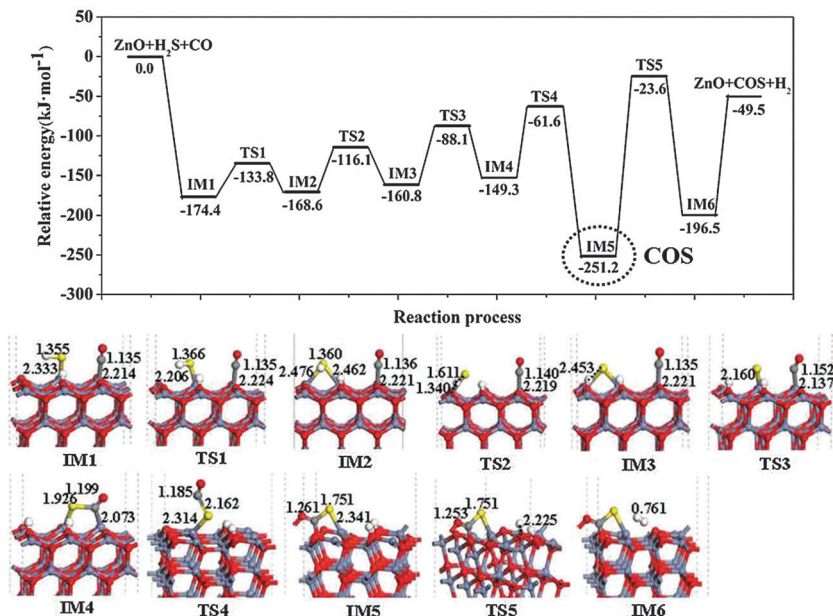


Fig. 3 Schematic potential energy profiles for the reaction of CO and H₂S on the ZnO(10 $\bar{1}$ 0) surface, as well as the corresponding structures of intermediates and transition states.

original site at all times, and the dissociation of H₂S is the same as that on the clean ZnO(10 $\bar{1}$ 0) surface.²⁷ This shows that CO does not significantly affect the dissociation of H₂S on the ZnO surface.¹³ Up to this step, the surface active S is formed.

Next, the adsorbed S reacts with CO, one of the S–Zn bonds cleaves and the S–C bond forms, leading to IM4 through TS3 with an imaginary frequency of -112.03 cm^{-1} . The activation energy is 72.7 kJ mol^{-1} . It seems as if COS is formed in IM4. However, this adsorption configuration of COS interacting with two neighboring Zn atoms with a S–C bond is not obtained when single COS is placed at the Zn–Zn bridge site on the ZnO(10 $\bar{1}$ 0) surface, which implies that a more stable adsorption structure of COS exists. Furthermore, the transfer of COS from the Zn–Zn bridge site to the short Zn–O bridge site proceeds because the O site in the adjacent long Zn–O bond has been occupied by a H atom. The reaction energy for the step (IM4 \rightarrow IM5) is $-101.9\text{ kJ mol}^{-1}$, which shows that IM5 is a more stable isomer than IM4. In IM5, S–C and C–O bonds are 1.751 and 1.261 Å, respectively, which is similar to the stable adsorption in COS(c). The activation energy for this step is 87.7 kJ mol^{-1} , which is the highest energy barrier in the previous four steps. In fact, COS has been formed in this step, and the highest energy barrier at TS4 is overcome to form COS *via* the Langmuir–Hinshelwood mechanism during the H₂S desulfurization reaction in the presence of CO on the ZnO surface. This provides theoretical support for the experimental result of Sasaoka *et al.*,¹² and shows that COS is produced *via* the reaction between active surface S and CO.

Finally, the two adsorbed H atoms in the intermediate IM5 can undergo a H₂-forming process giving IM6 through TS5 with an imaginary frequency of -298.51 cm^{-1} . An energy barrier of 227.6 kJ mol^{-1} is needed to overcome, which shows that H₂-elimination is more difficult than the formation of COS.

COS and H₂ releasing from the ZnO surface is an endothermic process with 147.0 kJ mol^{-1} .

3.3 The reaction of CO₂ and H₂S

With regard to the reaction of CO₂ and H₂S, the potential energy profile is shown in Fig. 4, intermediates and transition states are also depicted. First, an energy of 157.3 kJ mol^{-1} is released for the co-adsorbed H₂S and CO₂, which is designated as IM1*, in which H₂S is dissociative and CO₂ maintains a nearly linear geometry on the ZnO(10 $\bar{1}$ 0) surface. Then, an activation energy of 33.8 kJ mol^{-1} is needed to transform CO₂ from the linear mode to a V-shape mode. The transition state TS1* has been confirmed with an imaginary frequency of -195.13 cm^{-1} corresponding to the vibration of the C–O_{surface} bond. Subsequently, the stable SH adsorption state is formed in IM3* through TS2* with an energy barrier of 34.5 kJ mol^{-1} . And then, the SH bond cleaves and its H moves to the surface O, leading to the formation of IM4* by overcoming an energy barrier of 67.7 kJ mol^{-1} at TS3*. Similarly, CO₂ does not affect the dissociation of H₂S.¹³

Subsequently, a *cis*-hydrogen thiocarbonate species (IM5*) is formed *via* TS4* by fusing adsorbed H, S and CO₂, requiring an activation energy of 124.9 kJ mol^{-1} . The thiocarbonate surface species has been investigated when H₂S and CO₂ interact on γ -alumina by infrared analysis, which thereby leads to the formation of carbonyl sulphide.⁵⁰ And then, the conversion of *cis*- to *trans*-hydrogen thiocarbonate (IM5* to IM6*) accompanied by O–H bond rotation takes place, and the reaction barrier for this isomeric process is 54.4 kJ mol^{-1} . The transition state TS5*, with an imaginary frequency of -345.24 cm^{-1} , occurs.

The H atom in the IM6* intermediate can undergo H-migration *via* a four-member ring transition state TS6* leading to IM7*. The activation energy is 142.4 kJ mol^{-1} . In this step, the C=O bond has been changed into a single bond following the H-migration,

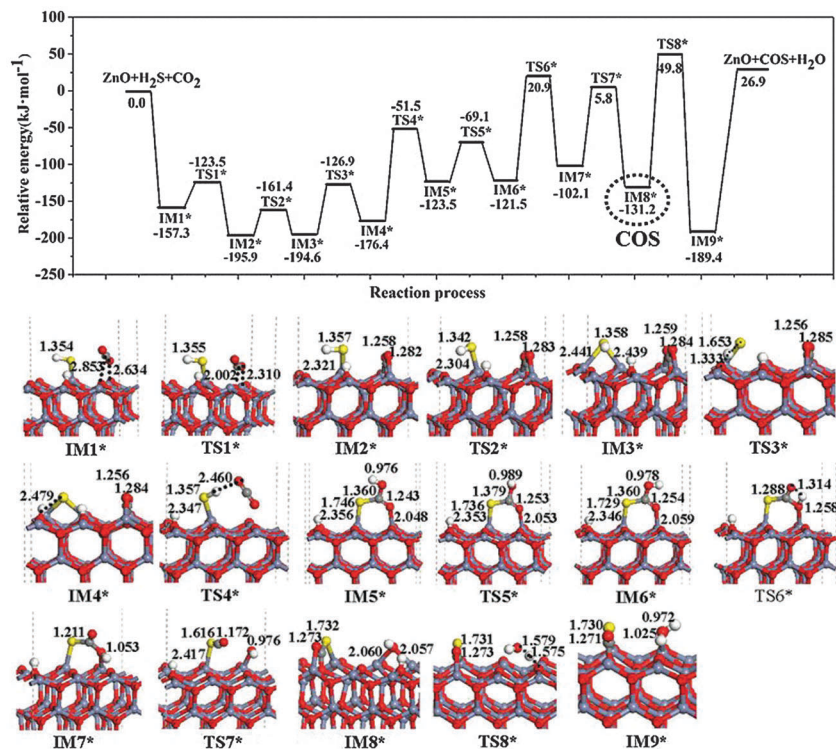


Fig. 4 Schematic potential energy profiles for the reaction of CO_2 and H_2S on the $\text{ZnO}(10\bar{1}0)$ surface, as well as the corresponding structures of intermediates and transition states.

and the formed new O–H bond is 1.053 Å long. Subsequently, the C–OH bond cleaves leading to the formation of COS in IM8^* , in which COS adsorbs onto a long Zn–O bridge site and O interacts with the adjacent Zn. An energy barrier of $107.9 \text{ kJ mol}^{-1}$ is needed in this step. In IM8^* , COS has been formed, the rate-determining step is $\text{IM6}^* \rightarrow \text{IM7}^*$ with an activation energy of $142.4 \text{ kJ mol}^{-1}$.

Finally, the adsorbed hydroxyl group will react with the surface H to form H_2O . With H transferring from the surface O to OH, an energy barrier of $181.0 \text{ kJ mol}^{-1}$ is needed *via* TS8^* with an imaginary frequency of -1671.95 cm^{-1} .

3.4 Thermodynamic and kinetic analyses of COS formation

The reaction of H_2S with CO and CO_2 over a ZnO catalyst can be described as follows:



It is known that the catalyst can only change the kinetics but not the thermodynamics of a reaction. The enthalpy correction (H') and Gibbs free energy correction (G') at different temperatures

will be determined by frequency analysis with the same parameters as the optimization. The detailed information on thermodynamic data for each species at 298.15, 500, 650 and 1000 K can be seen in the ESI† (Table S2), and the reaction enthalpy and the reaction Gibbs free energy for (R1) and (R2) can be obtained according to eqn (3) and eqn (4), which are summarized in Table 2. It can be concluded that the reaction of H_2S and CO leading to the formation of COS and H_2 is exothermic, and the Gibbs free energy below 650 K shows that this is a feasible reaction in thermodynamics.⁵¹ Nevertheless, the homogeneous reaction without a catalyst is negligible below 523 K,¹³ and our previous work shows that an activation energy of $249.5 \text{ kJ mol}^{-1}$ is needed for the rate-determining step during the reaction of H_2S and CO leading to the formation of COS and H_2 .⁵² As a consequence, a ZnO catalyst promotes the formation of COS during the removal of H_2S in the presence of CO. In addition, the Gibbs free energy changes from a negative to a positive number when the temperature changes from 298.15 to 1000 K, which shows that increasing temperature is disadvantageous to the reaction between H_2S and CO. For the formation of H_2O , the reaction is endothermic. The Gibbs free energy decreases with an increase in temperature, which implies that increasing temperature has a positive effect on the reaction

Table 2 Thermodynamic properties of reactions: $\text{H}_2\text{S} + \text{CO} \rightarrow \text{COS} + \text{H}_2$ and $\text{H}_2\text{S} + \text{CO}_2 \rightarrow \text{COS} + \text{H}_2\text{O}$ at different temperatures (K)

	$\Delta_r H_m$ (kJ mol ⁻¹)				$\Delta_r G_m$ (kJ mol ⁻¹)			
	298.15	500	650	1000	298.15	500	650	1000
$\text{H}_2\text{S} + \text{CO} \rightarrow \text{COS} + \text{H}_2$	-56.6	-56.6	-56.7	-57.6	-30.9	-13.5	-0.7	29.7
$\text{H}_2\text{S} + \text{CO}_2 \rightarrow \text{COS} + \text{H}_2\text{O}$	30.9	28.5	26.4	20.4	21.3	15.5	11.8	5.3

Table 3 The activation enthalpy, activation entropy and rate constant for the rate-determining step of formation of COS at different temperatures (K)

Rate-determining step	$\Delta_r H_m^\ddagger$ (kJ mol ⁻¹)			$\Delta_r S_m^\ddagger$ (J mol ⁻¹ K ⁻¹)			ln <i>k</i>		
	298.15	500	1000	298.15	500	1000	298.15	500	1000
IM4 → IM5	82.9	81.9	78.3	38.1	35.3	30.4	0.6	14.5	24.9
IM6* → IM7*	128.3	127.3	124.8	-5.7	-8.4	-11.8	-23.0	-1.6	14.2

between H₂S with CO₂. For the two reactions, the Gibbs free energy is greater than zero from approximately 650 to 1000 K, which shows from the thermodynamics that the formation of COS can be inhibited in this temperature range.

$$\Delta_r H_m = E(P) + H'(P) - E(R) - H'(R) \quad (3)$$

$$\Delta_r G_m = E(P) + G'(P) - E(R) - G'(R) \quad (4)$$

where $E(P)$ and $E(R)$ are electronic total energies of products and reactants, respectively. $H'(P)$ and $H'(R)$ are enthalpy correction of products and reactants at a certain temperature, which include vibrational, rotational and translational contributions, as well as zero-point vibration energy (ZPVE); and $G'(P)$ and $G'(R)$ are Gibbs free energy corrections of products and reactants at a certain temperature, which also include ZPVE vibrational, rotational and translational contributions.

Based on analysis of the geometry of every intermediate, we can see that COS has been formed in IM5 and IM8*. The kinetic data, including activation enthalpy $\Delta_r H_m^\ddagger$, activation entropy $\Delta_r S_m^\ddagger$ and rate constant ln *k* of the rate-determining step for the COS formation during the above two reactions, are calculated, and listed in Table 3. In addition, the enthalpy correction (H') and entropy (S) for each species at 298.15, 500 and 1000 K, which can be determined by frequency analysis with the same parameters as the optimization, are shown in Table S3 in the ESI.† According to the transition state theory, $\Delta_r H_m^\ddagger$, $\Delta_r S_m^\ddagger$ and *k* can be obtained from eqn (5), (6) and (7), respectively.

$$\Delta_r H_m^\ddagger = E(\text{TS}) + H'(\text{TS}) - E(\text{R}) - H'(\text{R}) \quad (5)$$

$$\Delta_r S_m^\ddagger = S(\text{TS}) - S(\text{R}) \quad (6)$$

$$k = \frac{k_b T}{h} \left(\frac{p^\theta}{RT} \right)^{1-n} \exp\left(\frac{-\Delta_r H_m^\ddagger}{RT} \right) \exp\left(\frac{\Delta_r S_m^\ddagger}{R} \right) \quad (7)$$

where^{53,54} $H(\text{TS})$ is the enthalpy correction of the transition state at the same temperature as that of the reactant; $S(\text{TS})$ and $S(\text{R})$ are entropies of the transition state and the corresponding reactant; *k* is the rate constant, *T* is the reaction temperature, k_b is the Boltzmann constant, *h* is Planck's constant, p^θ is the standard atmospheric pressure, *R* is the fundamental gas constant, and *n* is the number of reactants.

The rate constants ln *k* for the two steps are large, and it can be concluded that COS can be formed both in the presence of CO and CO₂ during the removal of H₂S by the ZnO catalyst. In addition, the reaction rate increases with an increase in temperature for both reactions. Moreover, the rate constant ln *k* for the step (IM4 → IM5) is larger than that of the step (IM6* → IM7*), which shows that the formation of COS in the presence of CO is easier than for CO₂. The same result has been obtained by Yang *et al.*,¹³ who believe that CO is more active than CO₂ in COS formation during

the desulfurization of H₂S using a ZnO sorbent by detecting COS concentration at a temperature of 673 K. As another important experiment also supports the above result,¹² it can be concluded that the formation of COS in the H₂S–CO–CO₂ system occurs from the commencement of the reaction of H₂S and ZnO, but that the formation of COS in the presence of CO₂ starts at *ca.* 3.5 h at 773 K.

It can be seen from the thermodynamic and kinetic analysis that kinetics is the main controlling factor for the formation of COS, as the rate constants for two reactions are large and COS has been investigated in the temperature range of 650–1000 K.^{12,13} Since the formation of COS is inevitable during the desulfurization of H₂S over ZnO, it is necessary to add a promoter to ZnO in order to remove COS. Recently, char-supported Fe–Zn–Cu and Fe–Zn–Mo sorbents have been prepared, which may simultaneously remove H₂S and COS from coke oven gas.^{55,56}

4. Conclusions

Using the DFT method, we carried out a periodic slab-model study to investigate the influence of CO and CO₂ during the desulfurization of H₂S on the ZnO(10 $\bar{1}$ 0) surface. The stable adsorption configurations of separated species (H₂S, H₂, CO, CO₂, COS and H₂O) were obtained, which were then employed to locate the co-adsorption structures. It was found that H₂S is adsorbed dissociatively on the ZnO(10 $\bar{1}$ 0) surface both independently and in the presence of CO and CO₂. There are two stable structures for COS adsorption on the ZnO(10 $\bar{1}$ 0) surface *via* S–C bond binding with either a long or a short Zn–O bond.

Thermodynamics shows that increasing temperature is favorable for the reaction of H₂S and CO₂, but unfavorable for the reaction of H₂S and CO. Kinetics is the main controlling factor for the formation of COS. The activation energy of the rate-determining step for the formation of COS *via* the interaction between the dissociated active S and CO is 87.7 kJ mol⁻¹, while it is 142.4 kJ mol⁻¹ for CO₂ combining with active S. The rate constants at different temperatures also show that the formation of COS in the presence of CO is easier than that of CO₂. The formation of COS is inevitable during the desulfurization of H₂S over ZnO, especially in the presence of CO. Therefore the addition of a promoter to ZnO in order to improve the desulfurization efficiency is necessary.

Acknowledgements

We gratefully thank Dennis for helping us revise the English language, and we acknowledge the National Natural Science Foundation of China (Grant No. 21276171 and 21576178), the National Younger Natural Science Foundation of China (Grant No. 21103120), the Program for the Innovative Talents of Higher

Learning Institutions of Shanxi, and the Wyoming Engineering Initiative in the U.S.

References

- 1 T. H. Ko, H. Chu, H. P. Lin and C. Y. Peng, *J. Hazard. Mater.*, 2006, **136**, 776–783.
- 2 M. Cal, B. Strickler and A. Lizzio, *Carbon*, 2000, **38**, 1757–1765.
- 3 Z. B. Huang, B. S. Liu, F. Wang and R. Amin, *Appl. Surf. Sci.*, 2015, **353**, 1–10.
- 4 P. J. Robinson and W. L. Luyben, *Ind. Eng. Chem. Res.*, 2010, **49**, 4766–4781.
- 5 K. Kim, S. Jeon, C. Vo, C. S. Park and J. M. Norbeck, *Ind. Eng. Chem. Res.*, 2007, **46**, 5848–5854.
- 6 H. S. Song, M. G. Park, E. Croiset, Z. Chen, S. C. Nam, H.-J. Ryu and K. B. Yi, *Appl. Surf. Sci.*, 2013, **280**, 360–365.
- 7 I. Rosso, C. Galletti, M. Bizzi, G. Saracco and V. Specchia, *Ind. Eng. Chem. Res.*, 2003, **42**, 1688–1697.
- 8 G. Qi, L. Zhang and Z. Yuan, *Phys. Chem. Chem. Phys.*, 2014, **16**, 13434–13439.
- 9 R. Portela, F. Rubio-Marcos, P. Leret, J. F. Fernández, M. A. Bañares and P. Ávila, *J. Mater. Chem. A*, 2015, **3**, 1306–1316.
- 10 A. Samokhvalov and B. J. Tatarchuk, *Phys. Chem. Chem. Phys.*, 2011, **13**, 3197–3209.
- 11 I. I. Novochinskii, C. Song, X. Ma, X. Liu, L. Shore, J. Lampert and R. J. Farrauto, *Energy Fuels*, 2004, **18**, 576–583.
- 12 E. Sasaoka, S. Hirano, S. Kasaoka and Y. Sakata, *Energy Fuels*, 1994, **8**, 1100–1105.
- 13 H. Yang, R. Sothen, D. R. Cahela and B. J. Tatarchuk, *Ind. Eng. Chem. Res.*, 2008, **47**, 10064–10070.
- 14 W. Xie, L. Chang, D. Wang, K. Xie, T. Wall and J. Yu, *Fuel*, 2010, **89**, 868–873.
- 15 M. Pineda, J. Palacios, L. Alonso, E. Garcia and R. Moliner, *Fuel*, 2000, **79**, 885–895.
- 16 J. Yu, L. Chang, W. Xie and D. Wang, *Korean J. Chem. Eng.*, 2011, **28**, 1054–1057.
- 17 L. Ling, M. Fan, B. Wang and R. Zhang, *Energy Environ. Sci.*, 2015, **8**, 3109–3133.
- 18 J. Martins, C. Taft, E. Longo and J. Andres, *THEOCHEM*, 1997, **398**, 457–466.
- 19 M. Casarin, C. Maccato and A. Vittadini, *Appl. Surf. Sci.*, 1999, **142**, 192–195.
- 20 M. Casarin, C. Maccato and A. Vittadini, *Inorg. Chem.*, 1998, **37**, 5482–5490.
- 21 J. Martins, C. Taft, S. Lie and E. Longo, *THEOCHEM*, 2000, **528**, 161–170.
- 22 J. B. Lopes Martins, E. Longo, O. D. Rodríguez Salmon, V. A. A. Espinoza and C. A. Taft, *Chem. Phys. Lett.*, 2004, **400**, 481–486.
- 23 W. Chen, Y. Zhang, K. Ding, Y. Xu, Y. Li and J. Li, *Chin. J. Struct. Chem.*, 2004, **23**, 337–341.
- 24 M. Casarin, C. Maccato and A. Vittadini, *Surf. Sci.*, 1997, **377**, 587–591.
- 25 M. Casarin, C. Maccato, E. Tondello and A. Vittadini, *Surf. Sci.*, 1995, **343**, 115–132.
- 26 J. A. Rodriguez and A. Maiti, *J. Phys. Chem. B*, 2000, **104**, 3630–3638.
- 27 L. Ling, R. Zhang, P. Han and B. Wang, *Fuel Process. Technol.*, 2013, **106**, 222–230.
- 28 L. Ling, P. Han, B. Wang and R. Zhang, *Fuel Process. Technol.*, 2013, **109**, 49–56.
- 29 L. Ling, P. Han, B. Wang and R. Zhang, *Chem. Eng. J.*, 2013, **231**, 388–396.
- 30 L. Ling, J. Wu, J. Song, P. Han and B. Wang, *Comput. Theor. Chem.*, 2012, **1000**, 26–32.
- 31 A. Wander and N. Harrison, *Surf. Sci.*, 2000, **457**, L342–L346.
- 32 N. Marana, V. Longo, E. Longo, J. Martins and J. Sambrano, *J. Phys. Chem. A*, 2008, **112**, 8958–8963.
- 33 J. Hu, W.-P. Guo, X.-R. Shi, B.-R. Li and J. Wang, *J. Phys. Chem. C*, 2009, **113**, 7227–7235.
- 34 B. Meyer and D. Marx, *Phys. Rev. B: Condens. Matter Mater. Phys.*, 2003, **67**, 035403.
- 35 H. Hu, Z. Lv, S. Cui and G. Zhang, *Chem. Phys. Lett.*, 2011, **510**, 99–103.
- 36 J. P. Perdew, K. Burke and M. Ernzerhof, *Phys. Rev. Lett.*, 1996, **77**, 3865–3868.
- 37 J. P. Perdew, K. Burke and Y. Wang, *Phys. Rev. B: Condens. Matter Mater. Phys.*, 1996, **54**, 16533.
- 38 P. Hohenberg and W. Kohn, *Phys. Rev.*, 1964, **136**, B864–B871.
- 39 R. Zhang, H. Liu, H. Zheng, L. Ling, Z. Li and B. Wang, *Appl. Surf. Sci.*, 2011, **257**, 4787–4794.
- 40 B. Delley, *J. Chem. Phys.*, 1990, **92**, 508–517.
- 41 B. Delley, *J. Chem. Phys.*, 2000, **113**, 7756–7764.
- 42 T. A. Halgren and W. N. Lipscomb, *Chem. Phys. Lett.*, 1977, **49**, 225–232.
- 43 J. Lin, J. May, S. Didziulis and E. Solomon, *J. Am. Chem. Soc.*, 1992, **114**, 4718–4727.
- 44 K. D'amico, F. McFeely and E. I. Solomon, *J. Am. Chem. Soc.*, 1983, **105**, 6380–6383.
- 45 R. R. Gay, M. H. Nodine, V. E. Henrich, H. Zeiger and E. I. Solomon, *J. Am. Chem. Soc.*, 1980, **102**, 6752–6761.
- 46 Q. Yuan, Y.-P. Zhao, L. Li and T. Wang, *J. Phys. Chem. C*, 2009, **113**, 6107–6113.
- 47 A. Aboulayt, F. Mauge, P. Hoggan and J. Lavalley, *Catal. Lett.*, 1996, **39**, 213–218.
- 48 Y. Yan and M. M. Al-Jassim, *Phys. Rev. B: Condens. Matter Mater. Phys.*, 2005, **72**, 235406.
- 49 A. Calzolari and A. Catellani, *J. Phys. Chem. C*, 2009, **113**, 2896–2902.
- 50 J.-C. Lavalley, J. Travert, T. r. s. Chevreau, J. Lamotte and O. Saur, *J. Chem. Soc., Chem. Commun.*, 1979, 146–148.
- 51 F. Faraji, I. Safarik, O. P. Strausz, M. E. Torres and E. Yildirim, *Ind. Eng. Chem. Res.*, 1996, **35**, 3854–3860.
- 52 R. Zhang, L. Ling and B. Wang, *J. Mol. Model.*, 2010, **16**, 1911–1917.
- 53 C. Frisch, A. R. Fersht and G. Schreiber, *J. Mol. Biol.*, 2001, **308**, 69–77.
- 54 X. Fu, W. Shen, T. Yao and W. Hou, *Physical Chemistry*, Higher Education Press, Beijing, 2010, 243.
- 55 J. Dou, A. Tahmasebi, X. Li, F. Yin and J. Yu, *Environ. Prog. Sustainable Energy*, 2016, **35**, 352–358.
- 56 J. Dou, X. Li, A. Tahmasebi, J. Xu and J. Yu, *Korean J. Chem. Eng.*, 2015, **32**, 2227–2235.